Catalysis Today 434 (2024) 114705

Contents lists available at ScienceDirect

Catalysis Today

journal homepage: www.elsevier.com/locate/cattod

Catalytical advantages of Hf-MOFs in benzaldehyde acetalization

Elena García-Rojas [a], Jesús Tapiador [a], Pedro Leo [a], Carlos Palomino [b], Carmen Martos [a,*], Gisela Orcajo [a]

[a] Chemical and Environmental Engineering Group. ESCET, Rey Juan Carlos University, C/Tulipán s/n, Móstoles 28933, Spain
[b] Department of Chemistry, University of the Balearic Islands, Cra. de Valldemossa, 07122, Spain

ARTICLE INFO

Keywords:
UiO-66
MOF-808
Acetalization
Benzaldehyde
Metal-organic frameworks
Acid sites

ABSTRACT

The potential use of acetals as bioadditives based on sustainable feedstocks in the automotive industry is of great interest. If such feedstock is a residual stream, the process would represent a dual environmental challenge, such as the valorization of glycerol obtained as a by-product of biodiesel to produce acetals. There are just scarce works about this synthetic route due to the challenge in finding efficient catalytic converters for glycerol valorization in a single process. Herein four different Metal-Organic Frameworks (MOFs) are evaluated as heterogeneous catalysts for the acetalization reaction of benzaldehyde with methanol, specifically, two structures, MOF-808 and UiO-66, containing two structural metal ions, zirconium and hafnium. The aim of this work is to investigate the influence of the MOF structure, the metallic active sites and the reaction conditions on the catalytic performance of this acetal production-type reaction. Furthermore, the recyclability of the catalyst is evaluated, and a potential reaction mechanism is suggested. As relevant results, Hf-MOFs showed higher benzaldehyde conversion than Zr-based ones, and significant improvements in reaction conditions were achieved, such as a significant reduction in catalyst loading of 99.6 % using UiO-66-Hf, and an optimization of reagent ratios reducing methanol consumption by 50 % for a 92 % of benzaldehyde conversion. The Brønsted character of UiO-66-Hf seems to enhance the reaction rate more than the metal center accessibility and larger pore volumes offered by MOF-808.

1. Introduction

Acetals have their main application in the chemical, fine chemical cosmetics and pharmaceutical industries as intermediates or final compounds [1]. However, these products are becoming increasingly important in the automotive industry as well since they can be used as bioadditives for oxygenated fuels to increase the octane number of gasoline [2,3], improve the properties of biodiesel [4,5] and even to reduce particulate emissions [6,7]. The reaction mechanism of acetal production involves two reversible steps, through the reaction of two alcohol molecules with one of aldehyde, which is catalyzed by an acid, either Lewis or Brønsted. In the first step, an alcohol molecule reacts with an aldehyde molecule, leading to the formation of the corresponding hemiacetal. In the second step, another alcohol molecule reacts with the hydroxyl group of the hemiacetal to form the corresponding acetal and water [8,9]. In recent years, acetal production in industry has largely increased, which involves the use of homogeneous catalysts such as H_2SO_4, HF, HCl, H_3PO_4 [10–13]. However, these catalytic processes have notable drawbacks since there are severe corrosion problems, large volume of toxic wastes produced as well as the common problems catalysts recovery [14]. To address these issues, heterogeneous catalysis could be implemented in this kind of processes. So far, several types of materials have been tested as heterogeneous acid catalysts for the acetalization of diverse carbonyl compounds, including activated carbons [15,16], zeolites [17,18], montmorillonite [19,20], heteropolyacids with a Keggin structure [21], graphene oxide [22], polyoxometalate [23] and acidic resins such as Amberlyst [24,25].

Metal-Organic Frameworks (MOFs) are porous, crystalline, and versatile materials, formed by metal ions or cluster nodes and functional organic ligands, connected through coordination bonds [26,27]. Due to their structural versatility, MOFs can harbor Lewis and Brønsted acid sites that enhance their properties as a heterogeneous catalyst [28–31]. The acetalization of benzaldehyde with methanol using different MOFs as heterogenous catalysts have been recently tested [32–35]. In 2010, Dhakshinamoorthy et al. reported a MOF structure in this reaction for the first time [32], demonstrating that it provides higher activity for

* Corresponding author.
E-mail address: carmen.martos@urjc.es (C. Martos).

https://doi.org/10.1016/j.cattod.2024.114705
Received 2 November 2023; Received in revised form 15 February 2024; Accepted 6 April 2024
Available online 10 April 2024

acetal formation compared to zeolites and clays.

Shortly after, Timofeeva and others produced a series of closely related MOFs using the UiO-66 design [33]. Their objective was to investigate the impact that the linking functional groups had on Lewis acidity in solids through inductive effects. They discovered that enhanced Lewis acidity resulted in a higher catalytic activity in acetalization. More recently in 2020, Hall et al. noted that Brønsted acid sites generated a more significant catalytic activity for the acetalization reaction in MIL-100(Cr) and MIL-100(Fe) materials [35]. However, it remains unclear whether the catalytic performance of the reaction is governed by Lewis or Brønsted acids, despite the utilization of diverse structures featuring distinct metal ions.

So far, the few MOFs that have been studied and reported in literature show that the highest catalytic performance in acetalization has been achieved employing the UiO-66-Zr structure [33,34,36]. In this regard, a series of MOFs with 12-, 10-, 8-, and 6-connected nodes have been described elsewhere due to the versatility of Zr-based nodes as structural elements. For instance, MOF-808-Zr has displayed higher catalytic activity compared to UiO-66-Zr in several reactions [37,38]. In both structures the same secondary building unit (SBU) of $Zr_6O_4(OH)_4$ is connected to twelve 1,4-benzene-dicarboxylate (BDC) ligands in UiO-66, whereas six benzene-1,3,5-tricarboxylic acid (BTC) ligands are attached to an SBU in MOF-808, so the coordinatively units are unsaturated in MOF-808-Zr, resulting in the terminal Zr-OH/Zr-OH_2 being oriented towards the center of the MOF pores. This, along with its improved textural properties, enhances the accessibility of the substrates to its active catalytic sites [39]. In this context, Gan Ye et al. have recently assessed the catalytic performance of MOF-808-Zr in this reaction using various synthesis methods [40], although it has not been compared to other MOF structures under the same conditions.

It is noteworthy that the similarity between zirconium and hafnium provides an opportunity to create isostructural materials for both MOF structures (MOF-808 and UiO-66) by simply substituting Zr for Hf reagents under similar synthetic conditions, while maintaining elevated high chemical, thermal and mechanical stability [41–44]. This is interesting as the same structure synthetized with dissimilar metals may exhibit different Lewis or Brønsted acid character, affecting catalytic performance and providing scope for further investigation [45].

In this work, the influence of the MOF structure, as well as the presence of zirconium and hafnium as metals in the UiO-66 and MOF-808 materials is evaluated in the acetalization reaction of benzaldehyde with methanol at room temperature. The effect of the reaction variables such as catalyst concentration and reactant ratios will be studied to determine the best operation conditions for the acetalization of benzaldehyde. Furthermore, this assessment allows an indirect comparison of the acidity of this two MOFs, highlighting the first testing of MOFs with structural hafnium ions in this reaction. Finally, the catalyst's recyclability is also evaluated through several successive catalytic runs, checking its structural and catalytic activity resistance.

2. Experimental section

2.1. Materials

All reagents and solvents were purchased from commercial sources and used without further purification. Benzaldehyde (BA, 99 %, Fluka), methanol (MeOH, >99.8 %, Merck), zirconium (IV) chloride ($ZrCl_4$, >99.5 %, Aldrich), hafnium (IV) chloride ($HfCl_4$, Alfa Aesar), dimethylformamide (DMF, >99 %, Cymit), formic acid (HCOOH, 90 %, Fisher Chemical), benzene-1,3,5-tricarboxylic acid (H_3BTC, >95 %, Aldrich), terephthalic acid (H_2BDC, 98 %, Aldrich), nitrobenzene (Aldrich).

2.2. Catalyst preparation

2.2.1. Synthesis of MOF-808-Zr

This material was synthesized following a procedure similar to that described by Y. Liu et al. [46]. $ZrCl_4$ (5 mmol, 1.165 g) and H_3BTC (5 mmol, 1.1 g) were dissolved in a mixture of DMF/HCOOH (200 mL/200 mL) and stirred for 30 min. The mixture was placed in an autoclave reactor at 100 °C for 72 h. The obtained white MOF powder was centrifuged and washed with fresh DMF and acetone, each solvent being used three times. Finally, it was dried in an oven at 100℃ for 6 h.

2.2.2. Synthesis of MOF-808-Hf

MOF-808-Hf was synthesized according to a previously reported procedure with minor modifications [47]. $HfCl_4$ (5 mmol, 1.63 g) was dissolved in a mixture of H_2O/HCOOH (30 mL/20 mL) and stirred at room temperature until a translucent solution was obtained. Then, H_3BTC (5 mmol, 1.05 g) ligand was added. The flask containing this mixture was placed in an oil bath with refluxed at 100 °C for 12 h. The white MOF powder obtained was centrifuged and washed three times with water and methanol. Finally, the material was dried in an oven at 100℃ for 6 h.

2.2.3. Synthesis of UiO-66-Zr

In a typical procedure, UiO-66-Zr material is prepared according to a method reported in the literature [48]. $ZrCl_4$ (164 mg, 0,7 mmol) and H_2BDC (114 mg, 0,7 mmol) were dissolved in 8 mL of DMF and were stirred for 30 min in a screw capped bottle. Then, the mixture was placed in an oven at 120℃ for 24 h. The white product obtained was washed with DMF and methanol twice. Finally, the MOF was dried in an oven at 100℃ for 6 h.

2.2.4. Synthesis of UiO-66-Hf

In a typical solvothermal synthesis [44], $HfCl_4$ (300 mg, 0,94 mmol) and H_2BDC (174 mg, 1 mmol) were dissolved in 10 mL of DMF solution containing 0.1 M H_2O and stirred for 30 min in a screw capped bottle. The synthesis was carried out in a pre-heated oven at 100℃ for 24 h. The resultant powder was centrifuged and washed out with fresh DMF and ethanol three times. Finally, it was dried in an oven at 100℃ for 6 h.

2.3. Instrumentation

X-ray powder diffraction (XRD) patterns were acquired on a PHILIPS XPERT PRO diffractometer using CuKα radiation (1.542 Å). The data were recorded from 5 to 50 (2θ) with a resolution of 0.01°. Argon adsorption–desorption isotherms were measured at 87 K using an 3Flex Micromeritics equipment, prior the samples were degassed at 150 °C and high vacuum during 12 h. The total surface area was calculated by using the Brunauer–Emmett–Teller (BET) model. Pore volume was assessed using the Dubinin-Radskevich equations. The pore size distribution was estimated using non-local DFT calculations, assuming a kernel model of split pore, Ar-carbon at 87 K. External surface was estimated by the t-plot method and the Harkins Jura equation. Simultaneous thermogravimetry and derivative thermogravimetric analyses (TGA/DTG) were carried out under air atmosphere at a heating rate of 5 °C/min up to 800 °C, using a SDT 2860 apparatus. Metal content in the filtered solution after reaction was measured by ICP–OES analysis collected in a Varian VISTA AX system. The acidity of the samples was investigated by CD_3CN adsorption at room temperature and CO adsorption at 77 K followed by FTIR spectroscopy using a Bruker Vertex 80 v spectrophotometer working at 3 cm^{-1} resolution. Commonly, a self-supporting wafer of MOF was prepared and degassed inside an IR cell under dynamic vacuum at 453 K for 8 h. The morphology of the samples was studied by Scanning Electron Microscopy (SEM) using a JEOL JSM-7900 F microscope with an accelerating voltage of 15 kV.

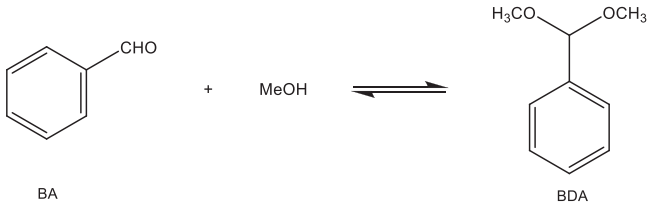

Scheme 1. Acetalization of benzaldehyde with methanol.

2.4. Reaction procedure

According to Scheme 1, the acetalization of benzaldehyde with methanol was carried out following the conditions described in previously published references [32–35]. 1 mmol of BA, 3 mL of methanol and 50 mg of MOF were added to a round bottom flask closed with a septum plug. This mixture was placed in a water bath at 30 °C to produce benzaldehyde dimethyl acetal (BDA).

For the kinetic studies, several aliquots were taken during the reaction (2 h). All samples were analyzed three times by gas chromatography (Fig. S2.1.), using a GC-3900 Varian chromatograph equipped with a HP-5 column (30 m × 0.25 mm, film thickness 0.25 μm) and a flame ionization detector (FID). Prior to injection, nitrobenzene was added to each sample as an internal standard. The catalytic turnover number, TON = mmol of product/mmol of metal in the catalyst, is measured at different times to evaluate the activity of the metallic sites. Experimental metal content was estimated from TGA analysis. The turnover frequency, TOF=TON/time (h), was evaluated only at shorter times.

3. Result and discussion

3.1. Catalyst physicochemical characterization

To confirm the successful synthesis of the four materials (UiO-66-Zr, UiO-66-Hf, MOF-808-Zr, MOF-808-Hf), they were physiochemically characterized. Powder X-ray diffraction (XRD) patterns (Fig. S1.1.) show the location and the relative intensity of the main reflections

Table 1
Textural properties of MOF-808 and UiO-66.

Material	S_{BET}[a] (m^2/g)	S_{μ}[b] (m^2/g)	$S_{meso+Ext}$[b] (m^2/g)	V_P[c] (cm^3/g)	D_P[d](Å)	$mmol_{Me}/g_{cat}$[e]	%Me[f]	%Me[g]
UiO-66-Zr	1324	1216	108	0.43	10.9 and 7.5	3.70	32.9	33.7
UiO-66-Hf	833	627	206	0.40	11.5 and 7.5	2.84	49.0	50.7
MOF-808-Zr	2159	1596	563	0.71	16.8 and 21.7	4.35	40.1	39.7
MOF-808-Hf	998	561	437	0.57	13 and 17.9	3.00	56.7	53.1

[a] Specific surface area using- BET equation.
[b] Surface areas corresponding to microporosity and mesopores + external, calculated using the t-Plot method.
[c] Total pore volume at P/P_0=0.98.
[d] Pore diameter.
[e] mmol metal/g catalyst calculated by TGA analysis.
[f] Weight percent metal from the theorical molecular formula.
[g] Weight percent metal from the TGA residue.

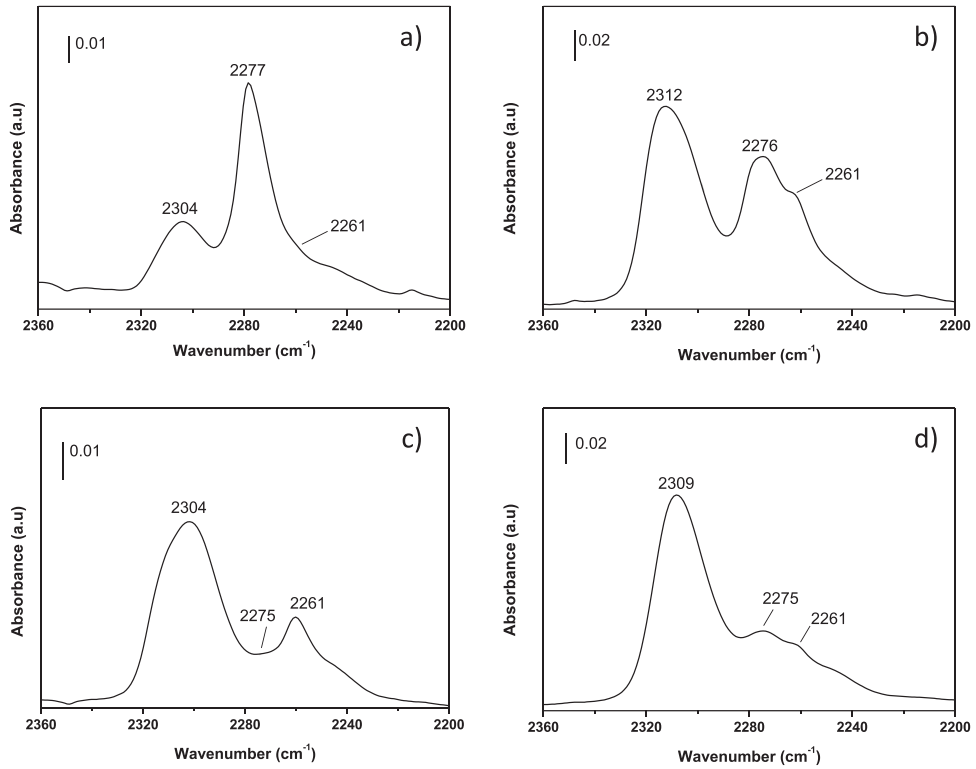

Fig. 1. FTIR spectra of CD_3CN adsorbed at 298 K on (a) UiO-66-Zr, (b) UiO-66-Hf, (c) MOF-808-Zr and (d) MOF-808-Hf.

corresponding to MOF-808 (8.3–8.7°, 9.9° and 10.9°) and UiO-66 (7.4° and 8.5°) crystalline structures [46,48]. When compared to the simulated pattern from the crystallographic data, no secondary crystalline phases are detected, confirming the exclusively presence of both the desired phases and isostructural MOFs with zirconium and hafnium ions. Both metals belong to the same group IV of the periodic table and have the same d^0 electronic configuration like Zr^{4+} and Hf^{4+}, and also have similar ionic radius, 79 and 78 pm respectively. Despite falling in a lower period than the lanthanide contraction, they have similar physical properties and coordination topologies[49–51].

Air TGA were performed from 50 to 800°C (Fig. S1.2) to study the thermal stability of these materials. Generally, three weight loss steps were observed. The first between 50 and 150°C, corresponding to removal of exchange solvent and moisture adsorbed from the porous system. The second weight loss was observed between 150 and 350°C, corresponding to the elimination of the solvent coordinated in the structure. The last weight loss is related to organic degradation and structural collapse. This study allowed the quantification of the metals contained in each of the materials as shown in Table 1.

Argon adsorption/desorption isotherms were performed to evaluate the textural properties of all MOF structures (Fig. S1.3). BET surface area, pore volume, and pore diameter are summarized in Table 1 which are found to be quite like those reported in literature [44,46–48], being higher in the case of MOF-808 structure with both metals. Increasing the connectivity of the $M_6O_4(OH)_4$ clusters from 6 to 12 changes the degrees of freedom from slightly flexible MOF-808 to rigid UiO-66 [52].

Scanning electron microscopy was carried out to study the morphology and particle size of four synthesized MOFs (Fig. S1.4). Hafnium materials have a spherical morphology, while MOF-808-Zr and UiO-66-Zr are different, being more similar to bipyramids and flakes, respectively. Hf-based MOFs were in the nanometer range while Zr ones were larger in the micrometer scale, following the order UiO-66-Hf < MOF-808-Hf < UiO-66-Zr < MOF-808-Zr, with average sizes of 90 nm, 130 nm, 700 nm and 1.02 μm, respectively.

3.2. Lewis and Brønsted acid-sites characterization

The nature of the acid sites of the prepared catalyst was assessed by FTIR spectroscopy using CD_3CN and CO as probe molecules. The IR spectra of CD_3CN adsorbed on all activated samples (Fig. 1) shows two ν(CN) vibrational bands at 2312−2304 and 2261 cm^{-1}, assigned to the adsorption of CD_3CN on Lewis acid sites and to physiosorbed CD_3CN, respectively [53]. A comparison of the frequencies of the bands corresponding to CD_3CN adsorbed on Lewis acid sites shows that these bands appear on the Hf-MOFs at a higher wavenumber than on the spectra of the Zr-MOFs, indicating a stronger Lewis acidity of Hf-MOFs, which has been also observed by other authors [54].Adsorption of CD_3CN also clearly revealed the existence of Brønsted acid sites through ν(CN) bands at 2277−2275 cm^{-1} [53,54]. The normalized integrated signals associated with Brønsted and Lewis acid sites of all the studied MOFs indicated that the catalyst with the highest and lowest number of acid sites are UiO-66-Hf and MOF-808-Zr, respectively (Fig. S1.5). On the other hand, Fig. S1.6. shows the IR spectra in the ν(CO) region of adsorbed CO on activated catalysts. The infrared spectra of adsorbed CO on UiO-66 samples show a distinctive IR absorption band at 2152 cm^{-1} associated with OH−CO interaction. Which is in agreement with previous results [55]. It should be noted that carbon monoxide is a weaker base than acetonitrile and, in the case of MOF-808 samples, no interaction was observed, which suggests a higher Brønsted acid strength of UiO-66 catalysts.

3.3. Catalytic activity

The initial study was performed using the reaction conditions reported in literature: 1 mmol of benzaldehyde (BA), 3 mL of methanol and 50 mg of catalyst were added at room temperature with vigorous stirring for 24 h [33]. Zirconium and hafnium MOF-808 were used as catalyst to evaluate the influence of the metal ion on the reaction (Fig. 2). Although MOF-808-Zr has been previously evaluated [40], its isostructural hafnium counterpart has not been tested in the acetalization reaction of benzaldehyde with methanol, despite the significant potential of the metal ion in this application.

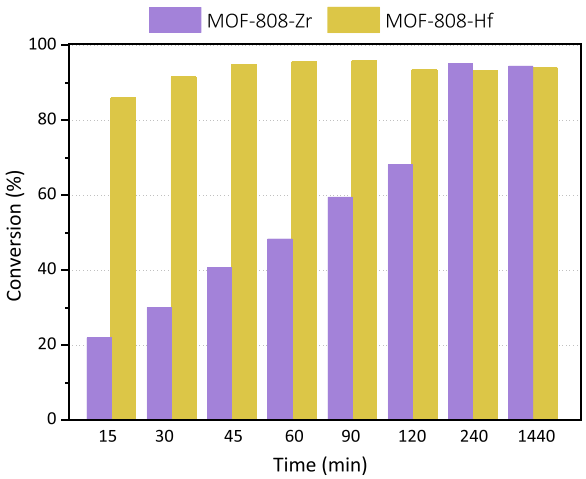

Fig. 2. Benzaldehyde conversion of MOF-808 structure with Zr and Hf.

Table 2
TON of MOF-808 of Zr and Hf. Reaction condition: 50 wt% of MOF, benzaldehyde (1 mmol), methanol (75 mmol) and 30°C.

time (min)	MOF-808-Hf	MOF-808-Zr
15	5.6	1.0
30	6.0	1.4
45	6.2	1.8
60	6.2	2.2
90	6.3	2.7
120	6.1	3.1
240	6.1	4.3
1440	6.1	4.3

After 24 h, similar results were obtained for both materials, but significant differences in the performance of the reaction were observed. When Hf was used, the initial reaction rate is significantly faster, reaching a conversion of 85 % in 15 min, compared to 21 % for the Zr-MOF catalyst. In order to compare the individual effect of the catalytic metal sites of each material on the performance in the acetalization reaction, the TON was calculated and shown in Table 2, confirming what has been observed in terms of conversion. Furthermore, for 15 min, the hafnium material exhibits a TOF of 22 $mmol \cdot g^{-1} \cdot h^{-1}$ versus 4 $mmol \cdot g^{-1} \cdot h^{-1}$ for zirconium. It is supposed that textural properties are not a critical parameter in these catalytic experiments since a large amount of catalysts is added to the reaction media, so it is expected a high availability of the active centers. This result could be related to the higher Brønsted acidity of Hf ions compared to Zr ones in isostructural MOF materials [37], that has been attributed to a slightly higher oxophilicity of the former. For example, Bakuru et al. tested isostructural UiO-66 MOFs based on Zr, Ce and Hf in the acetalization of glycerol with acetone, observing remarkable differences in the reaction conversion related to the metal ion's oxophilicity [45]. This behavior has been explained by the higher dissociation enthalpy of the Hf-O bond (802 KJ/mol) versus Zr-O bond (776 KJ/mol), which confers a stronger Brønsted acid character to the former [56]. The stronger Lewis character of Hf produces a higher polarization of the Hf-O bond, which might contribute to the Brønsted acidity of Hf-containing structures, which is in agreement with the results found in the characterization of the acid sites through FITR using CD_3CN as a molecule probe. It should be noted

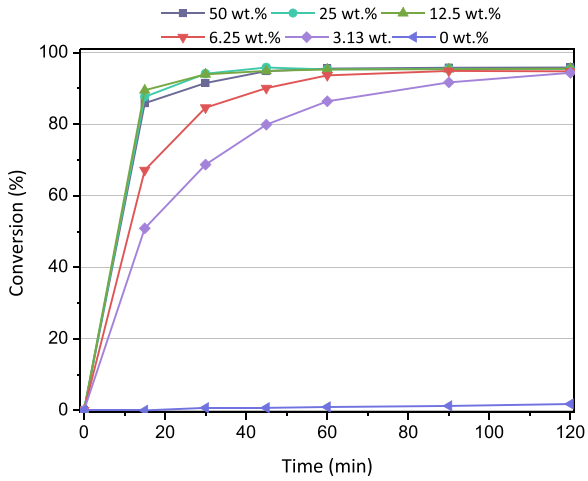

Fig. 3. Study of catalyst loading of MOF-808-Hf in acetalization of benzaldehyde with methanol. Reaction conditions: benzaldehyde (1 mmol), methanol 3 mL (75 mmol) and 30°C.

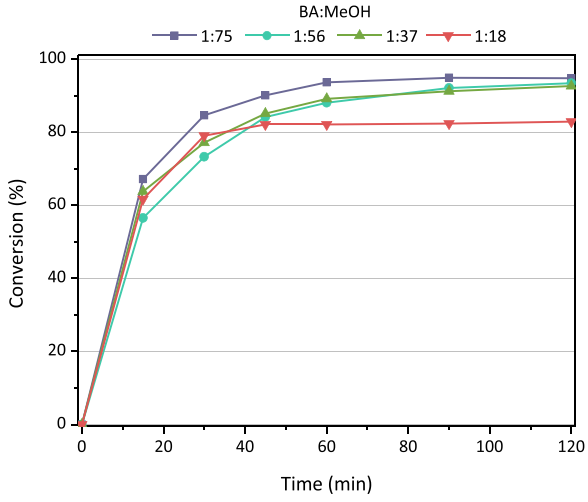

Fig. 4. Influence of reagents molar ratio in acetalization of benzaldehyde with methanol. Reaction conditions: 6.25 wt% MOF-808-Hf and 30°C.

that in all cases, the selectivity obtained was 100 %, and the only product observed was benzaldehyde dimethyl acetal with no reaction by-product, followed by ^{1}H-RMN (Fig. S2.2.).

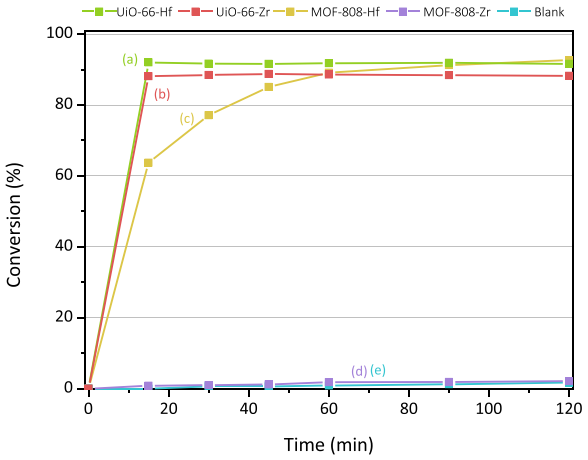

Fig. 6. Conversion profiles for benzaldehyde acetalization, catalyzed by (a) 6.25 wt% UiO-66-Hf; (b) 6.25 wt% UiO-66-Zr; (c) 6.25 wt% MOF-808-Hf; (d) 6.25 wt% MOF-808-Zr and (e) blank (no catalyst). Reaction condition: benzaldehyde (1 mmol), methanol (37 mmol) and 30°C.

3.4. Optimization of reaction parameters

Based on the high benzaldehyde conversion obtained with MOF-808-Hf, the reaction conditions were optimized for this material by varying the catalyst loading and reagents ratio. The first reaction variable studied was the catalyst loading, starting with the value of 50 wt% used elsewhere [33], with respect to the limiting reagent (benzaldehyde), and reducing it until a significant decrease in the BA conversion was observed (Fig. 3). The BA conversion rate was not significatively reduced up to a catalyst loading of 6.25 %. Even at the lower catalyst loading tested (3.13 %), a 95 % BA conversion was achieved in two hours. The outstanding results demonstrate that by using the highly active MOF-808-Hf, the catalyst loading can be significantly reduced even for shorter reaction times without affecting the reaction kinetics, resulting in a great economic saving. Fig. 3 also shows a blank reaction (without catalyst), indicating that no conversion can be detected in this case, highlighting the essential role of the MOF catalyst in this reaction.

The other variable to be optimized in this study was the reagent ratio. For this set of experiments a 6.25 wt% catalyst loading of MOF-808-Hf was fixed. The initial reagent BA:MeOH molar ratio was 1:75, and it was gradually reduced (Fig. 4). This molar ratio between the reactants has been studied with the aim of reducing the excess of MeOH, which also acts as a solvent. This reduction would represent obvious economic and environment advantages. When a 1:18 molar ratio was tested, the reaction stabilized after 45 min with a maximum conversion of 85 %.

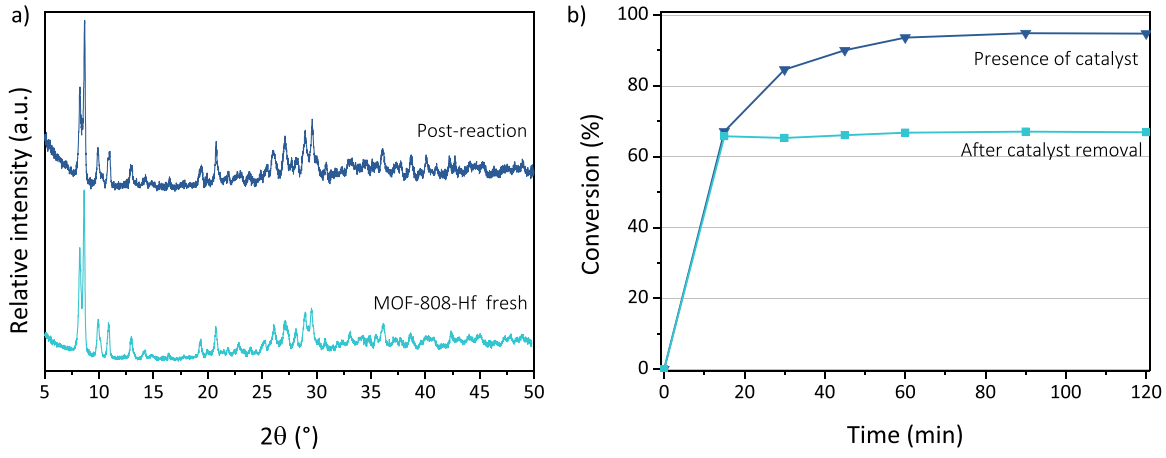

Fig. 5. a) XRD patterns of MOF-808-Hf before and after reaction. b) Leaching test.

Table 3
TON of various catalyst. Reaction condition: 6.25 wt% of MOF, benzaldehyde (1 mmol), methanol (37 mmol) and 30°C.

time (min)	UiO-66-Hf	MOF-808-Hf	UiO-66-Zr	MOF-808-Zr
15	50.8	35.1	37.4	0.3
30	50.6	44.2	37.5	0.4
45	50.6	47.1	37.7	0.4
60	50.7	48.9	37.6	0.7
90	50.7	49.6	37.5	0.7
120	50.6	49.5	37.4	0.8

When the molar ratio was set at 1:37, adjust slight difference in BA conversion after 1 h of reaction was observed, 89 % vs 94 % respect to those obtained with the maximum excess of methanol. Because of this small drop of 5 % in conversion, the best conditions were stablished at 6.25 wt% MOF-808-Hf and 1:37 molar ratio of reagents.

The stability of the material in the reaction media was checked, Fig. 5a shows that the crystalline phase of MOF-808-Hf remained similar after the reaction and a leaching test was carried out (Fig. 5b), where the MOF catalyst was filtered after 15 min, without obtaining any increase in the conversion. Finally, excluding the leaching of active species capable of homogeneous catalysis, no Hf was detected in the reaction media by ICP-OES analysis. These facts suggest that the reaction proceeds by a heterogeneous catalytic mechanism.

Once the best reaction conditions for MOF-808-Hf had been determined, the study was extended to UiO-66 structure with Zr and Hf (Fig. 6). Surprisingly, UiO-66 achieved 94 % BA conversion in 15 min under these conditions. This was an unexpected result because MOF-808 is less coordinated and has a larger pore volume, so the metal center should be more accessible [39,57]. Based on the SEM images (Fig. S1.4.), UiO-66 has smaller particle sizes compared to MOF-808 and, therefore a larger external surface area should be expected, which could favor catalytic performance as fewer diffusion constraints could be found. However, the results of the *t-plot* analysis provide larger values of the sum of external surface area and mesoporous area for MOF-808 because this material has cavities in the near mesoporosity range. Thus, even with an opener structure, MOF-808 showed a lower activity. For a possible explanation of these findings, it is essential to evaluate the acidic properties of both, however this task is not straightforward. Several researchers agree that MOFs based on Zr or Hf oxoclusters often exhibit Brønsted acidity, which is related to strongly polarized H_2O molecules adsorbed on Zr^{4+} or Hf^{4+} sites and it is more pronounced in UiO-66 than in MOF-808 [58,59], as described above for CD_3CN and CO FTIR results. Thus, the Brønsted character of the UiO-66 material has a higher effect over the reaction performance than the better accessibility to the metal centres of the MOF-808 material when these two materials are compared under more stringent conditions. Therefore, the results derived from this study can be considered as an indirect measure of the Brønsted acidity between these MOF materials.

Once again, the TON has been calculated and shown in Table 3 to compare the individual effect of the catalytic metal sites of each material in performing the acetalizing reaction. In terms of mass, UiO-66 structures offer higher conversions than MOF-808 ones (Fig. 6), but in terms of TON (per metal center), the trend changes, finding UiO-66-Hf > MOF-808-Hf > UiO-66-Zr > MOF-808-Zr.This result confirms that hafnium-based MOFs give better results than their zirconium counterparts, as seen in previous experiments, but also that Hf in MOF-808 structure is even more active than UiO-66-Zr, showing higher impact the metal ion over the MOF structure. To further emphasize the differences between the materials, the TOF was calculated at 15 and 30 min, being 203, 140, 150 and 1.2, and 101, 88, 75 and 0.7 for UiO-66-Hf, MOF-808-Hf, UiO-66-Zr and MOF-808-Zr respectively. At lower times, it shows that UiO-66 converts more BA than MOF-808 per active site; so MOF-808-Hf led to a worse performance at both reaction times in spite of its larger surface area.

Once these four materials were compared, the catalytic activity of

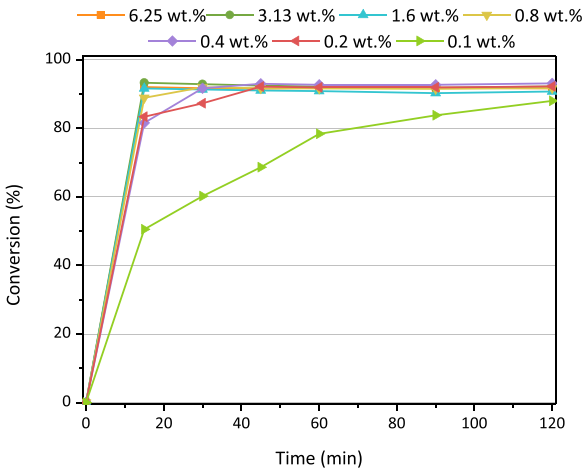

Fig. 7. Optimization catalyst loading of UiO-66-Hf in acetalization of benzaldehyde with methanol. Reaction conditions: benzaldehyde (1 mmol), methanol (37 mmol), different catalyst loading and 30°C.

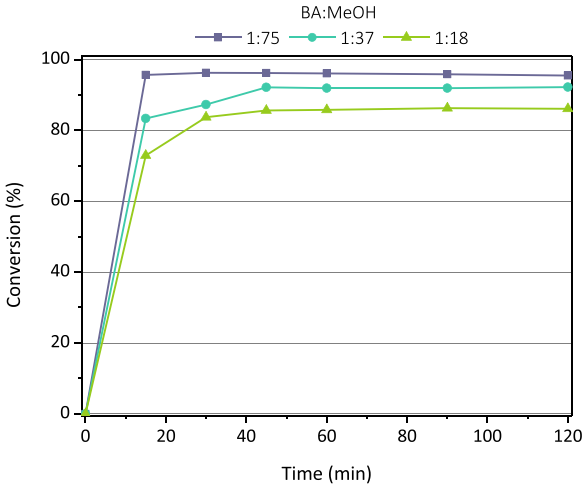

Fig. 8. Influence of reagent molar ratio in acetalization of benzaldehyde with methanol. Reaction conditions: 0.2 wt% UiO-66-Hf, different reagent ratio and 30°C.

their precursors were tested. In this sense, zirconium tetrachloride ($ZrCl_4$), hafnium tetrachloride ($HfCl_4$), and both the organic linkers, benzene dicarboxylic acid (BDC) and benzene tricarboxylic acid (BTC) were added to the reaction media with a concentration of 6.25 wt%, these results are shown in Figure S3.1. A conversion of 85 % for $HfCl_4$ and 76 % for $ZrCl_4$ was observed after 15 min, showing the catalytic role of the metal. However, it should be noted, that these salts are partially soluble in the reaction medium, as measured by ICP-OES, so these salts are giving rise to homogeneous catalysis. Finally, when organic ligands were tested, much lower conversions were obtained: 41 % for BTC and 9 % for BDC. The presence of the MOF catalysts is therefore a clear advantage, since they are more active and the reaction takes place rapidly and in a heterogeneous phase, that is easily recycled.

The catalyst loading was again optimized for UiO-66-Hf due to the faster kinetics observed for this catalyst. This parameter was progressively reduced compared to the best conditions obtained by optimizing MOF-808-Hf, as it is shown in Fig. 7. Firstly, a reduction of 99.6 % was reached respect to the 50 wt% catalyst loading used in the literature conditions, using a catalyst loading of 0.2 wt%, obtaining a similar BA conversion for the best conditions using MOF-808-Hf, even at shorter times. When 0.1 wt% of UiO-Hf loading was used, a sharp decrease in reaction rate was observed. It should be note that the reaction set was

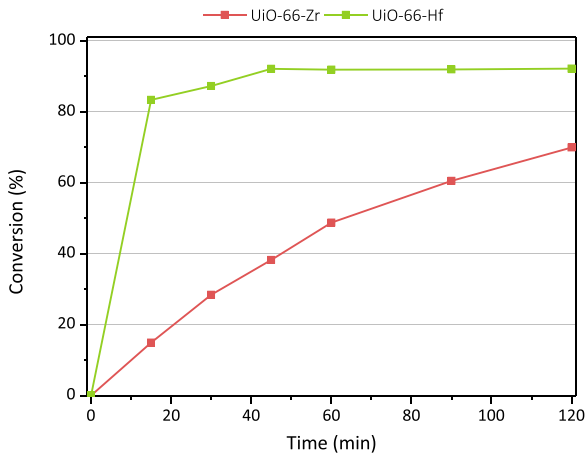

Fig. 9. Conversion of benzaldehyde acetalization catalyzed by 0.2 wt% of catalyst. Reaction conditions: benzaldehyde (1 mmol), methanol (37 mmol) and 30°C.

Table 4
TON of UiO-66 of Zr and Hf. Reaction condition: 0.2 wt% of MOF, benzaldehyde (1 mmol), methanol (37 mmol) and 30°C.

time (min)	UiO-66-Hf	UiO-66-Zr
15	1473	202
30	1542	385
45	1628	519
60	1623	661
90	1624	821
120	1629	949

scaled up to minimize the weight error.

In this case, the reagent ratio was also evaluated (Fig. 8). UiO-66-Hf was fixed at 0.2 wt%, varying the reagent molar ratio BA:MeOH between 1:75 and 1:18. Again, an appropriate excess of methanol is required to avoid the use of solvents. When the molar ratio was decreased to 1:35, a similar BA conversion was reached. However, when the lower molar ratio (1:18) was employed, a significant reduction in BA conversion was observed. So, the optimized reaction conditions were 0.2 wt% of UiO-66-Hf and a molar reagent ratio of 1:35.

Finally, to compare the activity of Hf ions with Zr ions in the UiO-66 structure, both materials were tested under the best reaction conditions defined above (Fig. 9). As expected, the reaction kinetics was faster with Hf, which shows how the oxophilic nature of Hf has a decisive influence on the course of the reaction, confirming the results obtained when comparing the catalytic activity between both metal ions.

Table 4 shows the TON values for both materials, again demonstrating the outstanding catalytic activity of Hf in this reaction, regardless of the reaction time employed.

To verify the stability of UiO-66 Hf during the reaction, ICP-OES and powder XRD analyses were performed (Fig. 10a), which confirmed that the crystalline phase of the catalyst was preserved. A leaching test was also carried out (Fig. 10b), where the MOF catalyst was filtered after 15 min and no increase in the conversion was obtained. Moreover, no Hf species were detected in the reaction media by ICP-OES, thus demonstrating the stability of this material.

Finally, in Table 5, the works reported in the literature on the acetalization reaction of benzaldehyde with methanol using MOFs are listed for the purpose of comparison. In general, although the reaction conditions are not exactly the same in all the reported studies, it can be outlined that the results obtained herein for UiO-66-Hf are quite outstanding in terms of low catalyst concentration and fast kinetics.

3.5. Recyclability study

Recyclability is a key feature of heterogeneous catalysts, so it was

Table 5
Catalytic performance of benzaldehyde acetalization and methanol over various MOFs.

Entry	Catalyst	Time (h)	Conversion (%)	Ref.
1[a]	Fe(BTC)	2; 24	49; 71	[32]
2[a]	$Cu_3(BTC)_2$	2; 24	63;88	[32]
3[a]	$Al_2(BDC)_3$	24	66	[32]
4[a]	Cr(BDC)	1.5	73	[60]
5[a]	UiO-66-Zr	4,5; 24	50: 100	[33]
6[a]	UiO-66-NO_2-Zr	6	100	[33]
7[a]	UiO-66-Zr	0.25; 1; 24	86; 91; 83	[34]
8[a]	UiO-67-Zr	0.25; 1; 24	16; 85; 80	[34]
9[a]	UiO-66-DES	1	94	[36]
10[a]	UiO-66-DMF	1	93	[36]
11[b]	MOF-808 (Zr)-F	0.03	≈95	[40]
12[b]	MOF-808 (Zr)-S	0.03	≈ 0	[40]
13[c]	MOF-808-Hf	0.25;1	67; 93	This work
14[d]	UiO-66-Hf	0.25;1	83; 92	This work

[a] Reaction conditions: 50 mg of catalyst, 3 mL methanol (75 mmol), and 0.94 mmol of benzaldehydes at room temperature.
[b] 20 mg of catalyst, 10 mL methanol (75 mmol), and 4 mmol of benzaldehydes at 30 °C.
[c] 6.25 mg of catalyst, 3 mL methanol (37 mmol), and 1 mmol of benzaldehydes at 30 °C.
[d] 0.2 mg of catalyst, 3 mL methanol (37 mmol), and 1 mmol of benzaldehydes at 30 °C.

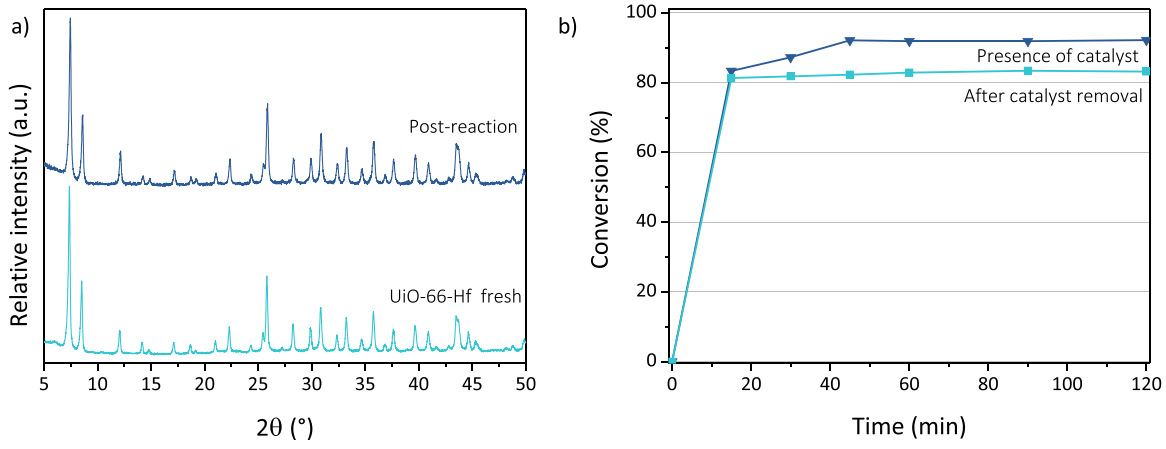

Fig. 10. a) XDR patterns of UiO-66-Hf before and after reaction. b) Leaching test.

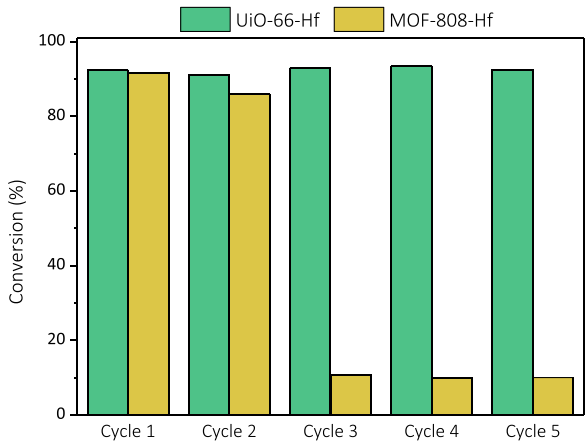

Fig. 11. Recyclability study with Hf-MOF. Reaction condition: 6.25 wt% of catalyst, benzaldehyde (1 mmol), methanol (37 mmol) and 30°C.

studied for the best Hf-MOFs evaluated in this work. These experiments were carried out under the best conditions found for MOF-808-Hf: 6.25 wt% MOF, benzaldehyde (1 mmol), methanol (37 mmol) and 30 °C for 90 min. After each cycle, the catalysts were just dried at 150°C for 30 min. The behavior of both materials was quite different. The UiO-66-Hf showed a stable catalytic activity over 5 cycles, indicating that this MOF is a suitable and stable solid acid catalyst for this acetalization reaction (Fig. 11). However, the MOF-808-Hf was only active during the first two cycles and then displayed a dramatic decrease in its catalytic activity afterwards.

Both materials were analyzed by XRD (Fig. 12), showing that the crystalline phase of both materials was maintained after the successive reactions. Considering also that no Hf was detected by ICP-OES, it can be concluded that the lost activity of MOF-808-Hf is not related to the damage of the material, but due to the catalyst deactivation that could come from the adsorption of the products on its exposed metal centres. For this purpose, a TGA analysis was carried out on this material, which profile is shown in Figure S4.1. The residue remaining after 520 °C is assumed to be HfO_2/$Hf(OH)_4$, which is larger in the fresh sample than in the recycled one (7.5 % difference). This expresses that the organic contribution is higher in the recycled sample, which may result from the strong adsorption effect of BDA reaction product, since the organic linker is the same in both samples.

3.6. Proposed mechanism for acetalization using UiO-66-Hf

A possible mechanism for the acetalization reaction of benzaldehyde and methanol using UiO-66-Hf is proposed in Fig. 13, based on a previous work by Ye et al. [40]. The oxygen atom of the benzaldehyde molecule interacts with a hydrogen atom of a hydroxyl group coordinated to Hf^{4+} (Step I). This H-O interaction increases the electrophilicity of the benzaldehyde carbon atom, which favors the nucleophilic attack of the oxygen atom of the methanol on the carbon atom of the carbonyl group present in the benzaldehyde molecule (Step II). The reaction intermediate then undergoes an intramolecular nucleophilic attack which results in the transfer of a hydrogen atom from the alcohol group to the oxygen atom in the aldehyde (Step III). A second molecule of methanol leads to a nucleophilic attack on the carbon atom of the benzaldehyde molecule, resulting in the release of an OH group (Step IV). Finally, this hydroxyl group takes the second hydrogen atom from the second molecule of methanol, producing a water molecule and the product of the reaction, the benzaldehyde dimethyl acetal (Step V).

4. Conclusions

Herein, two different MOF structures (UiO-66 and MOF-808) containing Zr and Hf ions were tested in the acetalization reaction of benzaldehyde with methanol The acidity of the four materials has been characterized by FTIR spectroscopy using in-situ absorption of acetonitrile and CO as probe molecules. In addition, the acidity of both metal ion and the MOF structure were key factors that controlled the overall reaction performance better than the textural properties of the catalyst. It was found that the oxophilic character of hafnium ions favors the benzaldehyde conversion. When comparing both Hf structures under the best conditions, it seems that the Brønsted acid character of the UiO-66 structure favored the reaction more than the higher accessibility of the metal center and larger pore volumes of MOF-808. Besides, the reaction conditions have been optimized for the first time, allowing a significant catalyst concentration reduction in the reaction media for both Hf-based MOF materials. The molar ratio of the reagents was also optimized, reducing the amount of methanol by 50 % and achieving similar yields in shorter times for both Hf-MOF catalysts. Finally, both materials were subjected to a recyclability study, where UiO-66-Hf maintained its catalytic activity for at least five reaction cycles, while MOF-808-Hf lost the activity drastically after two cycles, despite maintaining its crystalline structure and no Hf leaching was detected in the media, which may be related to BDA product adsorption effect on its exposed metal centers. This work opens to new routes of acetalization industrial applications using Hf-MOFs as effective catalysts.

CRediT authorship contribution statement

Gisela Orcajo: Conceptualization, Resources, Supervision, Writing –

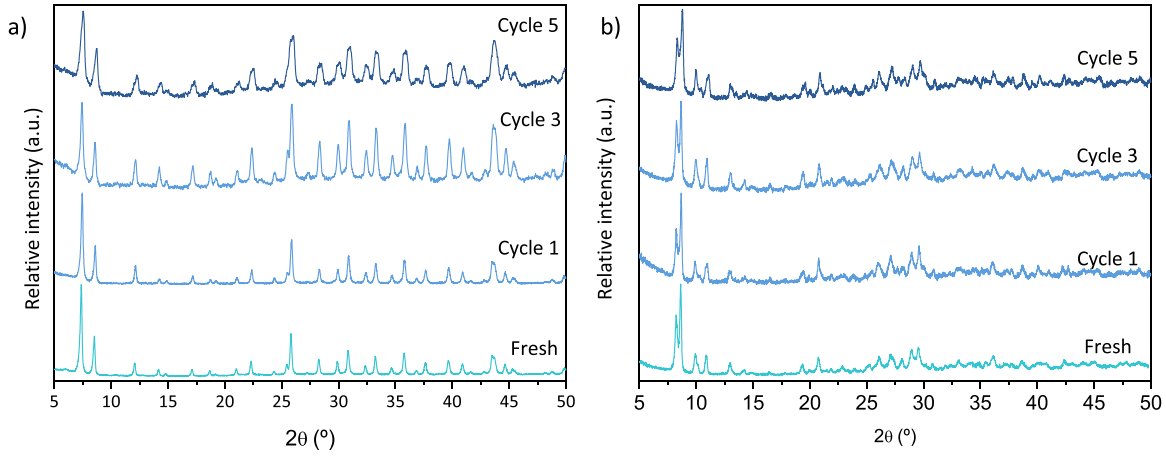

Fig. 12. XRD patterns of a) UiO-66-Hf and b) MOF-808-Hf before and after reaction cycle.

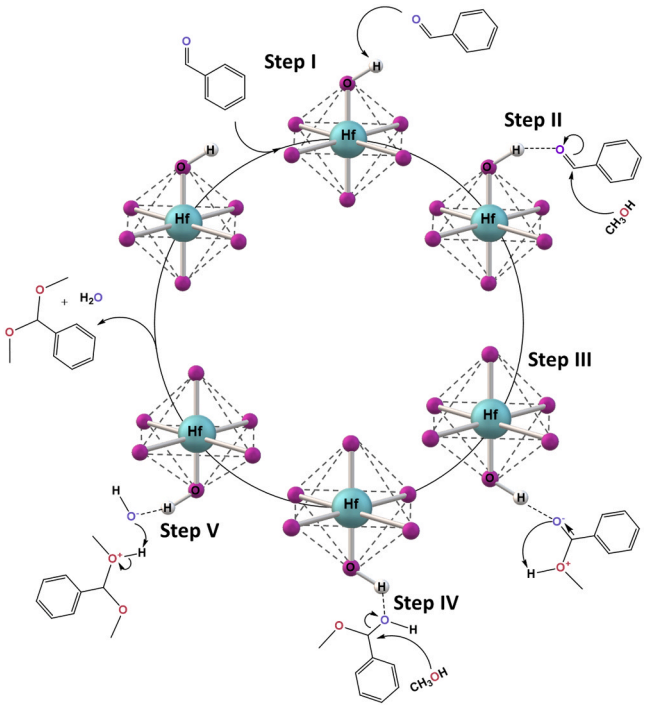

Fig. 13. Proposed mechanism of acetalization reaction of benzaldehyde and methanol using UiO-66-Hf.

review & editing. **Jesús Tapiador:** Methodology, Writing – original draft. **Elena García-Rojas:** Investigation, Writing – original draft. **Carlos Palomino:** Formal analysis, Investigation. **Pedro Leo:** Conceptualization, Methodology. **Carmen Martos Sanchez:** Conceptualization, Resources, Supervision, Writing – review & editing.

Declaration of Competing Interest

The authors declare the following financial interests/personal relationships which may be considered as potential competing interests: Gisela Orcajo reports financial support was provided by Spanish Ministry of Science and Innovation to the ECOCAT Project (PID2022-136321OA-C22). Gisela Orcajo reports financial support was provided by Rey Juan Carlos University. If there are other authors, they declare that they have no known competing financial interests or personal relationships that could have appeared to influence the work reported in this paper

Data availability

Data will be made available on request.

Acknowledgements

The authors gratefully acknowledge the financial support of Spanish Ministry of Science and Innovation to the ECOCAT Project (PID2022-136321OA-C22) and Universidad Rey Juan Carlos for IMPULSO and PUENTE Projects (grants MATER M-3000 and M-3032).

Appendix A. Supporting information

Supplementary data associated with this article can be found in the online version at doi:10.1016/j.cattod.2024.114705.

References

[1] M.B. Güemez, J. Requies, I. Agirre, P.L. Arias, V.L. Barrio, J.F. Cambra, Acetalization reaction between glycerol and n-butyraldehyde using an acidic ion exchange resin. Kinetic modelling, Chem. Eng. J. 228 (2013) 300–307, https://doi.org/10.1016/j.cej.2013.04.107.
[2] S.D. Varfolomeev, G.A. Nikiforov, V.B. Volieva, G.G. Makarov, L.I. Trusov, Agent for Increasing the Octane Number of Gasoline Automovile Fuel (2009).
[3] A. Smirnov, S. Selishcheva, V. Yakovlev, Acetalization catalysts for synthesis of valuable oxygenated fuel additives from glycerol, Catalysts 8 (2018) 595, https://doi.org/10.3390/catal8120595.
[4] P.H.R. Silva, V.L.C. Gonçalves, C.J.A. Mota, Glycerol acetals as anti-freezing additives for biodiesel, Bioresour. Technol. 101 (2010) 6225–6229, https://doi.org/10.1016/j.biortech.2010.02.101.
[5] E. García, M. Laca, E. Pérez, A. Garrido, J. Peinado, New class of acetal derived from glycerin as a biodiesel fuel component, Energy Fuels 22 (2008) 4274–4280, https://doi.org/10.1021/ef800477m.
[6] K.E. Nord, D. Haupt, Reducing the emission of particles from a diesel engine by adding an oxygenate to the fuel, Environ. Sci. Technol. 39 (2005) 6260–6265, https://doi.org/10.1021/es048085h.
[7] A. Aljaafari, I.M.R. Fattah, M.I. Jahirul, Y. Gu, T.M.I. Mahlia, Md.A. Islam, M. S. Islam, Biodiesel emissions: a state-of-the-art review on health and environmental impacts, Energies 15 (2022) 6854, https://doi.org/10.3390/en15186854.
[8] I. Agirre, V. Laura, M. Belen, J. Francisco, P. Luis, Acetals as possible diesel additives. in: Economic Effects of Biofuel Production, InTech, 2011, https://doi.org/10.5772/24440.
[9] J. Spitters, J.C. Gonçalves, R.P. v Faria, A.E. Rodrigues, Optimization of the production of 1,1-diethoxybutane by simulated moving bed reactor, Processes 9 (2021) 189, https://doi.org/10.3390/pr9020189.
[10] J.-L. Dong, L.-S.-H. Yu, J.-W. Xie, A simple and versatile method for the formation of acetals/ketals using trace conventional acids, ACS Omega 3 (2018) 4974–4985, https://doi.org/10.1021/acsomega.8b00159.
[11] S. Rudrawar, R. Besra, A. Chakraborti, Perchloric acid adsorbed on silica gel ($HClO_4$-SiO_2) as an extremely efficient and reusable catalyst for 1,3-dithiolane/dithiane formation, Synthesis 2006 (2006) 2767–2771, https://doi.org/10.1055/s-2006-942474.
[12] N. Hamada, K. Kazahaya, H. Shimizu, T. Sato, An efficient and versatile procedure for the synthesis of acetals from aldehydes and ketones catalyzed by lithium tetrafluoroborate, Synlett (2004) 1074–1076, https://doi.org/10.1055/s-2004-820038.
[13] B.T. Gregg, K.C. Golden, J.F. Quinn, Indium(III) trifluoromethanesulfonate as an efficient catalyst for the deprotection of acetals and ketals, J. Org. Chem. 72 (2007) 5890–5893, https://doi.org/10.1021/jo0707075.
[14] A.R. Trifoi, P. Agachi, T. Pap, Glycerol acetals and ketals as possible diesel additives. A review of their synthesis protocols, Renew. Sustain. Energy Rev. 62 (2016) 804–814, https://doi.org/10.1016/j.rser.2016.05.013.
[15] R. Rodrigues, M. Gonçalves, D. Mandelli, P.P. Pescarmona, W.A. Carvalho, Solvent-free conversion of glycerol to solketal catalysed by activated carbons functionalised with acid groups, Catal. Sci. Technol. 4 (2014) 2293–2301, https://doi.org/10.1039/C4CY00181H.
[16] M.S. Khayoon, B.H. Hameed, Solventless acetalization of glycerol with acetone to fuel oxygenates over Ni–Zr supported on mesoporous activated carbon catalyst, Appl. Catal. A Gen. 464–465 (2013) 191–199, https://doi.org/10.1016/j.apcata.2013.05.035.
[17] J. Kowalska-Kus, A. Held, M. Frankowski, K. Nowinska, Solketal formation from glycerol and acetone over hierarchical zeolites of different structure as catalysts, J. Mol. Catal. A Chem. 426 (2017) 205–212, https://doi.org/10.1016/j.molcata.2016.11.018.
[18] L. Roldán, R. Mallada, J.M. Fraile, J.A. Mayoral, M. Menéndez, Glycerol upgrading by ketalization in a zeolite membrane reactor, Asia Pac. J. Chem. Eng. 4 (2009) 279–284, https://doi.org/10.1002/apj.243.
[19] M.N. Timofeeva, V.N. Panchenko, V. v Krupskaya, A. Gil, M.A. Vicente, Effect of nitric acid modification of montmorillonite clay on synthesis of solketal from glycerol and acetone, Catal. Commun. 90 (2017) 65–69, https://doi.org/10.1016/j.catcom.2016.11.020.
[20] M.R. Nanda, Z. Yuan, W. Qin, H.S. Ghaziaskar, M.-A. Poirier, C. (Charles Xu, A new continuous-flow process for catalytic conversion of glycerol to oxygenated fuel additive: catalyst screening, Appl. Energy 123 (2014) 75–81, https://doi.org/10.1016/j.apenergy.2014.02.055.
[21] L. Liu, Q. Luan, J. Lu, D. Lv, W. Duan, X. Wang, S. Gong, 8-Hydroxy-2-methylquinoline-modified H4SiW12O40: a reusable heterogeneous catalyst for acetal/ketal formation, RSC Adv. 8 (2018) 26180–26187, https://doi.org/10.1039/C8RA04471F.
[22] A. Dhakshinamoorthy, M. Alvaro, M. Puche, V. Fornes, H. Garcia, Graphene oxide as catalyst for the acetalization of aldehydes at room temperature, ChemCatChem 4 (2012) 2026–2030, https://doi.org/10.1002/cctc.201200461.
[23] S. Zhao, Y. Jia, Y.-F. Song, Acetalization of aldehydes and ketones over $H_4[SiW_{12}O_{40}]$ and $H_4[SiW_{12}O_{40}]/SiO_2$, Catal. Sci. Technol. 4 (2014) 2618–2625, https://doi.org/10.1039/C4CY00021H.
[24] J. DEUTSCH, A. MARTIN, H. LIESKE, Investigations on heterogeneously catalysed condensations of glycerol to cyclic acetals, J. Catal. 245 (2007) 428–435, https://doi.org/10.1016/j.jcat.2006.11.006.
[25] A.L. Maximov, A.I. Nekhaev, D.N. Ramazanov, Ethers and acetals, promising petrochemicals from renewable sources, Pet. Chem. 55 (2015) 1–21, https://doi.org/10.1134/S0965544115010107.

[26] L. Jiao, J.Y.R. Seow, W.S. Skinner, Z.U. Wang, H.-L. Jiang, Metal–organic frameworks: structures and functional applications, Mater. Today 27 (2019) 43–68, https://doi.org/10.1016/j.mattod.2018.10.038.
[27] S. Abednatanzi, P. Gohari Derakhshandeh, H. Depauw, F.-X. Coudert, H. Vrielinck, P. van der Voort, K. Leus, Mixed-metal metal–organic frameworks, Chem. Soc. Rev. 48 (2019) 2535–2565, https://doi.org/10.1039/C8CS00337H.
[28] A. Bavykina, N. Kolobov, I.S. Khan, J.A. Bau, A. Ramirez, J. Gascon, Metal–organic frameworks in heterogeneous catalysis: recent progress, new trends, and future perspectives, Chem. Rev. 120 (2020) 8468–8535, https://doi.org/10.1021/acs.chemrev.9b00685.
[29] J. Guo, Y. Qin, Y. Zhu, X. Zhang, C. Long, M. Zhao, Z. Tang, Metal–organic frameworks as catalytic selectivity regulators for organic transformations, Chem. Soc. Rev. 50 (2021) 5366–5396, https://doi.org/10.1039/D0CS01538E.
[30] K. Rui, G. Zhao, Y. Chen, Y. Lin, Q. Zhou, J. Chen, J. Zhu, W. Sun, W. Huang, S. X. Dou, Hybrid 2D dual-metal–organic frameworks for enhanced water oxidation catalysis, Adv. Funct. Mater. 28 (2018) 1801554, https://doi.org/10.1002/adfm.201801554.
[31] A. Dhakshinamoorthy, Z. Li, H. Garcia, Catalysis and photocatalysis by metal organic frameworks, Chem. Soc. Rev. 47 (2018) 8134–8172, https://doi.org/10.1039/C8CS00256H.
[32] A. Dhakshinamoorthy, M. Alvaro, H. Garcia, Metal organic frameworks as solid acid catalysts for acetalization of aldehydes with methanol, Adv. Synth. Catal. 352 (2010) 3022–3030, https://doi.org/10.1002/adsc.201000537.
[33] M.N. Timofeeva, V.N. Panchenko, J.W. Jun, Z. Hasan, M.M. Matrosova, S. H. Jhung, Effects of linker substitution on catalytic properties of porous zirconium terephthalate UiO-66 in acetalization of benzaldehyde with methanol, Appl. Catal. A Gen. 471 (2014) 91–97, https://doi.org/10.1016/j.apcata.2013.11.039.
[34] U.S.F. Arrozi, H.W. Wijaya, A. Patah, Y. Permana, Efficient acetalization of benzaldehydes using UiO-66 and UiO-67: substrates accessibility or Lewis acidity of zirconium, Appl. Catal. A Gen. 506 (2015) 77–84, https://doi.org/10.1016/j.apcata.2015.08.028.
[35] J.N. Hall, P. Bollini, Metal–organic framework MIL-100 catalyzed acetalization of benzaldehyde with methanol: Lewis or Brønsted acid catalysis? ACS Catal. 10 (2020) 3750–3763, https://doi.org/10.1021/acscatal.0c00399.
[36] L. Chen, X. Ye, T. Zhang, H. Qin, H. Cheng, Z. Qi, Fast assembly of metal organic framework UiO-66 in acid-base tunable deep eutectic solvent for the acetalization of benzaldehyde and methanol, Molecules 27 (2022) 7246, https://doi.org/10.3390/molecules27217246.
[37] R.C. Klet, Y. Liu, T.C. Wang, J.T. Hupp, O.K. Farha, Evaluation of Brønsted acidity and proton topology in Zr- and Hf-based metal–organic frameworks using potentiometric acid–base titration, J. Mater. Chem. A Mater. 4 (2016) 1479–1485, https://doi.org/10.1039/C5TA07687K.
[38] E. Plessers, G. Fu, C. Tan, D. De Vos, M. Roeffaers, Zr-based MOF-808 as Meerwein–Ponndorf–Verley reduction catalyst for challenging carbonyl compounds, Catalysts 6 (2016) 104, https://doi.org/10.3390/catal6070104.
[39] S.-Y. Moon, Y. Liu, J.T. Hupp, O.K. Farha, InstantaneouS Hydrolysis of Nerve-agent Simulants with A Six-connected Zirconium-based Metal-organic Framework, Angew. Chem. Int. Ed. 54 (2015) 6795–6799, https://doi.org/10.1002/anie.201502155.
[40] G. Ye, L. Wan, Q. Zhang, H. Liu, J. Zhou, L. Wu, X. Zeng, H. Wang, X. Chen, J. Wang, BoostinG Catalytic Performance of MOF-808(Zr) by direct generation of rich defective Zr nodes via a solvent-free approach, Inorg. Chem. 62 (2023) 4248–4259, https://doi.org/10.1021/acs.inorgchem.2c04364.
[41] Y. Wang, Z. Hu, Y. Cheng, D. Zhao, Silver-decorated hafnium metal–organic framework for ethylene/ethane separation, Ind. Eng. Chem. Res. 56 (2017) 4508–4516, https://doi.org/10.1021/acs.iecr.7b00517.
[42] Z. Hu, A. Nalaparaju, Y. Peng, J. Jiang, D. Zhao, Modulated hydrothermal synthesis of UiO-66(Hf)-type metal–organic frameworks for optimal carbon dioxide separation, Inorg. Chem. 55 (2016) 1134–1141, https://doi.org/10.1021/acs.inorgchem.5b02312.
[43] X. Wang, L. Zhai, Y. Wang, R. Li, X. Gu, Y. di Yuan, Y. Qian, Z. Hu, D. Zhao, Improving water-treatment performance of zirconium metal-organic framework membranes by postsynthetic defect healing, ACS Appl. Mater. Interfaces 9 (2017) 37848–37855, https://doi.org/10.1021/acsami.7b12750.
[44] S. Jakobsen, D. Gianolio, D.S. Wragg, M.H. Nilsen, H. Emerich, S. Bordiga, C. Lamberti, U. Olsbye, M. Tilset, K.P. Lillerud, Structural determination of a highly stable metal-organic framework with possible application to interim radioactive waste scavenging: Hf-UiO-66, Phys. Rev. B 86 (2012) 125429, https://doi.org/10.1103/PhysRevB.86.125429.
[45] V.R. Bakuru, S.R. Churipard, S.P. Maradur, S.B. Kalidindi, Exploring the Brønsted acidity of UiO-66 (Zr, Ce, Hf) metal–organic frameworks for efficient solketal synthesis from glycerol acetalization, Dalton Trans. 48 (2019) 843–847, https://doi.org/10.1039/C8DT03512A.
[46] J. Xu, J. Liu, Z. Li, X. Wang, Y. Xu, S. Chen, Z. Wang, Optimized synthesis of Zr(IV) metal organic frameworks (MOFs-808) for efficient hydrogen storage, New J. Chem. 43 (2019) 4092–4099, https://doi.org/10.1039/C8NJ06362A.
[47] Z. Hu, T. Kundu, Y. Wang, Y. Sun, K. Zeng, D. Zhao, Modulated hydrothermal synthesis of highly stable MOF-808(Hf) for methane storage, ACS Sustain Chem. Eng. 8 (2020) 17042–17053, https://doi.org/10.1021/acssuschemeng.0c04486.
[48] S.J. Garibay, S.M. Cohen, Isoreticular synthesis and modification of frameworks with the UiO-66 topology, Chem. Commun. 46 (2010) 7700, https://doi.org/10.1039/c0cc02990d.
[49] K.O. Kirlikovali, Z. Chen, T. Islamoglu, J.T. Hupp, O.K. Farha, Zirconium-based metal–organic frameworks for the catalytic hydrolysis of organophosphorus nerve agents, ACS Appl. Mater. Interfaces 12 (2020) 14702–14720, https://doi.org/10.1021/acsami.9b20154.
[50] A.J. Howarth, A.W. Peters, N.A. Vermeulen, T.C. Wang, J.T. Hupp, O.K. Farha, Best practices for the synthesis, activation, and characterization of metal–organic frameworks, Chem. Mater. 29 (2017) 26–39, https://doi.org/10.1021/acs.chemmater.6b02626.
[51] M. Bosch, S. Yuan, H.-C. Zhou, Group 4 metals as secondary building units: Ti, Zr, and Hf-based MOFs. in: The Chemistry of Metal-Organic Frameworks: Synthesis, Characterization, and Applications, Wiley-VCH Verlag GmbH & Co. KGaA, Weinheim, Germany, 2016, pp. 137–170, https://doi.org/10.1002/9783527693078.ch6.
[52] Z. Hu, Y. Wang, D. Zhao, The chemistry and applications of hafnium and cerium (IV) metal–organic frameworks, Chem. Soc. Rev. 50 (2021) 4629–4683, https://doi.org/10.1039/D0CS00920B.
[53] S. Rojas-Buzo, B. Bohigues, C.W. Lopes, D.M. Meira, M. Boronat, M. Moliner, A. Corma, Tailoring Lewis/Brønsted acid properties of MOF nodes via hydrothermal and solvothermal synthesis: simple approach with exceptional catalytic implications, Chem. Sci. 12 (2021) 10106–10115, https://doi.org/10.1039/D1SC02833B.
[54] X. Feng, J. Hajek, H.S. Jena, G. Wang, S.K.P. Veerapandian, R. Morent, N. De Geyter, K. Leyssens, A.E.J. Hoffman, V. Meynen, C. Marquez, D.E. De Vos, V. Van Speybroeck, K. Leus, P. Van Der Voort, Engineering a highly defective stable UiO-66 with tunable Lewis- Brønsted acidity: the role of the hemilabile linker, J. Am. Chem. Soc. 142 (2020) 3174–3183, https://doi.org/10.1021/jacs.9b13070.
[55] K. Chakarova, I. Strauss, M. Mihaylov, N. Drenchev, K. Hadjiivanov, Evolution of acid and basic sites in UiO-66 and UiO-66-NH2 metal-organic frameworks: FTIR study by probe molecules, Microporous Mesoporous Mater. 281 (2019) 110–122, https://doi.org/10.1016/j.micromeso.2019.03.006.
[56] H. Beyzavi, R.C. Klet, S. Tussupbayev, J. Borycz, N.A. Vermeulen, C.J. Cramer, J. F. Stoddart, J.T. Hupp, O.K. Farha, A Hafnium-based metal−organicframework as an efficient and multifunctional catalyst for facile CO2 fixation and regioselective and enantioretentive epoxide activation, J. Am. Chem. Soc. 136 (2014) 15861–15864, https://doi.org/10.1021/ja508626n.
[57] H.-H. Mautschke, F. Drache, I. Senkovska, S. Kaskel, F.X. Llabrés i Xamena, Catalytic properties of pristine and defect-engineered Zr-MOF-808 metal organic frameworks, Catal. Sci. Technol. 8 (2018) 3610–3616, https://doi.org/10.1039/C8CY00742J.
[58] A. Rapeyko, M. Rodenas, F.X. Llabrés i Xamena, Zr-containing UiO-66 metal-organic frameworks as highly selective heterogeneous acid catalysts for the direct ketalization of Levulinic acid, Adv. Sustain Syst. 6 (2022) 2100451, https://doi.org/10.1002/adsu.202100451.
[59] F.G. Cirujano, F.X. Llabrés i Xamena, Tuning the catalytic properties of UiO-66 metal–organic frameworks: from Lewis to defect-induced Brønsted acidity, J. Phys. Chem. Lett. 11 (2020) 4879–4890, https://doi.org/10.1021/acs.jpclett.0c00984.
[60] A. Herbst, A. Khutia, C. Janiak, Brønsted instead of Lewis acidity in functionalized MIL-101Cr MOFs for efficient heterogeneous (nano-MOF) catalysis in the condensation reaction of aldehydes with alcohols, Inorg. Chem. 53 (2014) 7319–7333, https://doi.org/10.1021/ic5006456.